CARBON 59 (2013) 283–288

Available at www.sciencedirect.com

SciVerse ScienceDirect

journal homepage: www.elsevier.com/locate/carbon

3D microfabrication of single-wall carbon nanotube/polymer composites by two-photon polymerization lithography

Shota Ushiba [a], *Satoru Shoji* [a,*], *Kyoko Masui* [a], *Preeya Kuray* [b], *Junichiro Kono* [c], *Satoshi Kawata* [a]

[a] *Department of Applied Physics, Osaka University, 2-1 Yamadaoka, Suita, Osaka 565-0871, Japan*
[b] *Department of Materials Science and Engineering, Rutgers, The State University of New Jersey, Piscataway, NJ 08854, USA*
[c] *Department of Electrical and Computer Engineering, Rice University, Houston, TX 77005, USA*

ARTICLE INFO

Article history:
Received 13 November 2012
Accepted 9 March 2013
Available online 16 March 2013

ABSTRACT

We present a method to develop single-wall carbon nanotube (SWCNT)/polymer composites into arbitrary three-dimensional micro/nano structures. Our approach, based on two-photon polymerization lithography, allows one to fabricate three-dimensional SWCNT/polymer composites with a minimum spatial resolution of a few hundreds nm. A near-infrared femtosecond pulsed laser beam was focused onto a SWCNT-dispersed photo resin, and the laser light solidified a nanometric volume of the resin. The focus spot was three-dimensionally scanned, resulting in the fabrication of arbitrary shapes of SWCNT/polymer composites. SWCNTs were uniformly distributed throughout the whole structures, even in a few hundreds nm thick nanowires. Furthermore, we also found an intriguing phenomenon that SWCNTs were self-aligned in polymer nanostructures, promising improvements in mechanical and electrical properties. Our method has great potential to open up a wide range of applications such as micro- and nanoelectromechanical systems, micro/nano actuators, sensors, and photonics devices based on CNTs.

1. Introduction

Single-wall carbon nanotubes (SWCNTs) have attracted much attention because of their remarkable mechanical [1], electrical [2], thermal [3], and optical properties [4], as well as their unique chiral structure with extremely high aspect ratios. In particular, SWCNTs are promising as filler materials in polymer-based composites due to their ability to enhance the performance of matrices. It has been demonstrated that incorporation of SWCNTs into polymers enhances mechanical [5], electrical [6], and thermal properties [7], and therefore, SWCNT/polymer composites have opened up new device applications such as actuators [8,9], sensors [10], and photonic devices [11]. Furthermore, their small size makes it possible to design micro- or even sub-micro-sized SWCNT/polymer composites. Some progress has been made recently with fabrication of SWCNT/polymer composites in the form of micro/nano-films and fibers [12,13]. These composites have been fabricated through solution-blended [14], melt-blended [15], or in situ polymerization processing [16]. However, the conventional fabrication processes generally require solvent removal and/or high temperature treatment, resulting in distortions of fragile structures. Moreover, the fabrication processes are not applicable to three-dimensional (3D) micro/nano-fabrication because of lack of a spatial resolution. Therefore, there remains a huge challenge to achieve 3D micro/nano-fabrication of SWCNT/polymer composites. UV direct write fabrication has been proposed for 3D fabrication of SWCNT/polymer composites with a spatial resolution of sub-millimeters [17].

* *Corresponding author:* Fax: +81 6 6879 7330.
E-mail address: shoji@ap.eng.osaka-u.ac.jp (S. Shoji).
0008-6223/$ - see front matter
http://dx.doi.org/10.1016/j.carbon.2013.03.020

Here, we report on the development of 3D micro/nano-structural SWCNT/polymer composites with a spatial resolution of sub-micrometers by using the two-photon polymerization (TPP) lithography technique. TPP lithography has been well established as a powerful tool for developing arbitrary 3D fine polymer structures [18,19]. A near-infrared (NIR) pulsed laser beam tightly focused onto a photo-polymerizable monomer solidifies a nanometric volume of the monomer in the focus spot through TPP, and thus, arbitrary 3D micro/nano-sized polymer structures can be fabricated with a sub-diffraction-limit spatial resolution by scanning the focus spot three-dimensionally. Applications of the TPP lithography are extended to various research fields, such as photonic crystals [20,21], photonic quasicrystals [22], metamaterials [23,24], novel mechanical micro/nanostructures [25], microfluidics [26], functional micro/nano mechanical devices [27], cell culturing 3D scaffolds for tissue engineering [28], and novel platforms of optical data storage [29]. TPP lithography is also an ideal tool for developing nanomaterials/polymer composite based micro/nano-structures. Photoisomerizable dyes [30], semiconductor nanoparticles [31,32], metallic nanoparticles [33,34], and magnetic nanoparticles [35,36] provide additional physical properties in host polymers, achieving a variety of functional active micro/nano-devices.

Our approach described here is to disperse SWCNTs into an UV-curable monomer and fabricate micro/nano-structural SWCNT/polymer composites in the form of desired shapes by using TPP lithography. Since SWCNTs possess remarkable electrical, thermal, mechanical, and optical properties, we can expect significant enhancement of physical properties in polymer nanostructures. Thus, this approach for 3D micro/nano-fabrication of SWCNT/polymer composites is promising for functional applications in fields such as micro- and nanoelectromechanical systems (MEMS/NEMS) [27,37].

2. Experimental

2.1. *Preparation of SWCNT-dispersed photo resin*

SWCNTs, synthesized by the high-pressure carbon monoxide (HiPco) process at Rice University, and SWCNTs (HiPco Single-Wall Carbon nanotubes, Unidym) were used in this study (see Supplementary material; Supporting Fig. 1). SWCNTs were loaded into an acrylate monomer, R712 [38], provided from Nippon Kayaku Co., Ltd., at a ratio of 0.01 wt.%, and then dispersed by using sonicatior (250D-advanced, model # 101-063-837, Branson) for 1 h. Finally, photo-initiator (Benzil, Wako) and photo-sensitizer (2-benzyl-2-(dimethylamino)-4′-morpholinobutyrophenon, Aldrich) were loaded into the compound at a ratio of 1.67 and 1.67 wt.%, respectively, and the resin was subsequently stirred for a few minutes.

2.2. *Fabrication of 3D micro/nano structural SWCNT/polymer composites*

A Ti:sapphire femtosecond pulsed laser (Tsunami, Spectra-Physics, Newport Corp.) emitting at 780 nm, with a pulse width and a repetition rate of 100 fs and 82 MHz, respectively, was used as a light source. The laser beam was focused by an oil-immersion objective lens (100×, NA 1.4, Zeiss) onto the SWCNT-dispersed resin casted on a glass substrate which was placed on a three dimensional piezoelectric stage. The stage moved the resin relative to the focus spot according to programmed patterns. The typical laser intensity was 15 GW/cm^2. The exposure time was 4 ms at each scanning step controlled by a galvanometer shutter. After structures were created, unsolidified resin was rinsed away using acetone. The obtained structures were used for further characterization.

2.3. *Characterization of SWCNT-dispersed photo resin and SWCNT/polymer composites*

Absorption spectra were measured using UV–Vis-NIR spectrometer (UV-3600, Shimadzu) with sampling pitch of 0.5 nm. Scanning electron microscopy (SEM) observation was carried out using Field Emission-Scanning Electron Microscope (FE-SEM, JSM-6330F, JEOL). Before SEM observation, the samples were Osmium-coated with a thickness of a few nm using Osmium-coater (HPC-30W, Vacuum Device Inc.). Raman microscopy experiments were conducted using Raman microscope (Raman-11, Nanophoton Corp.) with an objective lens (100×, NA 0.9, Nikon). Two laser wavelengths of 532 and 785 nm were used for the excitation. Laser intensity and exposure time were optimized to take Raman spectra with sufficient signal to noise ratio.

3. Results and discussion

For TPP micro/nano-fabrication, it is essential to well-disperse SWCNTs in an UV-curable monomer because SWCNTs easily self-organize into bundles due to van der Waals interactions between the sidewalls of individual nanotubes [39]. We dispersed SWCNTs into an acrylate UV-curable monomer, R712 (Fig. 1a and see Section 2 for more details). Two benzene rings

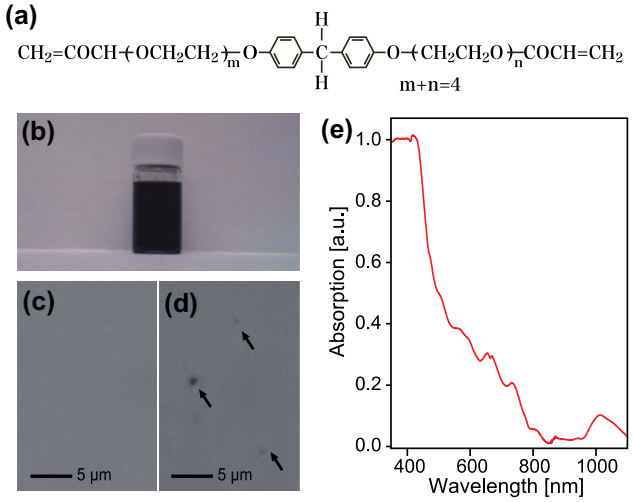

Fig. 1 – (a) The chemical structure of R712. (b) A photograph of the SWCNT-dispersed resin. (c) A bright field image of the SWCNT-dispersed resin. (d) A bright field image of the SWCNT-dispersed resin after 3 h from sonication. (e) An absorption spectrum of the SWCNT-dispersed resin.

in the monomer allow for π–π stacking interactions with graphitic sidewalls of SWCNTs, which leads to the stable dispersion of SWCNTs in the monomer. The bright field image of the SWCNT-dispersed photo-resin in Fig. 1c is optically flat, confirming that SWCNTs were isolated or formed small bundles in the photo-resin. Indeed, the SWCNTs were adequately dispersed for micro/nano fabrication. However, the dispersion did not last for a long time. After 3 h from sonication, SWCNTs started to form large bundles of ~1 μm indicated by the arrows in Fig. 1d. From this result, we carried out TPP lithography immediately within 3 h after the resin preparation. An absorption spectrum for the SWCNT-dispersed resin just after sonication is shown in Fig. 1e. The resin exhibits a strong optical absorption below 450 nm due to the π–π^* transition of electrons of SWCNTs as well as the absorption by the monomer. On the contrary, the resin shows relatively low absorption in the NIR range (>800 nm) although there are some small absorption peaks attributed to interband excitonic transitions in SWCNTs [40]. The appearance of intrinsic absorption peaks relevant to SWCNTs also implies that nanotubes were well dispersed in the resin.

Using the SWCNT-dispersed resin, we carried out micro/nano fabrication of SWCNT/polymer composites (see Section 2 for more details). The center wavelength of the Ti:sapphire femtosecond pulsed laser was tuned to 780 nm. This wavelength is suitable for the excitation of TPP of the photo-resin [18,19], and also corresponds to a valley between absorption peaks of SWCNTs, so that the excess absorption and/or damage of SWCNTs can be avoided. 3D micro/nano-structural SWCNT/polymer composites were fabricated based on programmed patterns, such as a 8-μm-long micro-bull, a micro-teapot, a micro-lizard, and a nanowire suspended between two micro boxes (Fig. 2a–f). The wire widths in lateral and vertical (along the laser beam propagation) directions are 300 and 800 nm, respectively. These results demonstrate that the fabrication technique exhibits the ability of 3D micro/nano-fabrication.

To determine whether SWCNTs are indeed embedded into the whole structures, Raman microscopy experiments were performed (Fig. 3). Fig. 3a shows a Raman spectrum taken from the box suspending the nanowire with an excitation wavelength of 785 nm. The Raman spectrum shows two specific peaks at 1595 and at 1300 cm^{-1} assigned to G-band and D-band of SWCNTs, respectively, providing evidence for the existence of SWCNTs in the polymeric structures. The Raman spectrum also shows some specific peaks in the range of 200–250 cm^{-1} assigned to RBM of SWCNTs, indicating that SWCNTs remain intact during the polymerization reaction. We also conclude that the Ti:sapphire laser beam did not cause any severe damage to the SWCNTs during the fabrication process, since the intensity ratio of G-band to D-band did not change between before and after TPP (Supporting Fig. 4). Raman images of the 300-nm-thick nanowire as well as two boxes, and a 8-μm-long micro-bull were reconstructed from the G-band intensity at each pixel in each bright field image (Fig. 3b–e). It should be noticed that the Raman scattering signal from the polymer was negligibly small compared to the SWCNT Raman signal due to resonant enhancement for SWCNTs under 785 nm excitation (Supporting Fig. 2a), and hence, the Raman images represent the distribution of

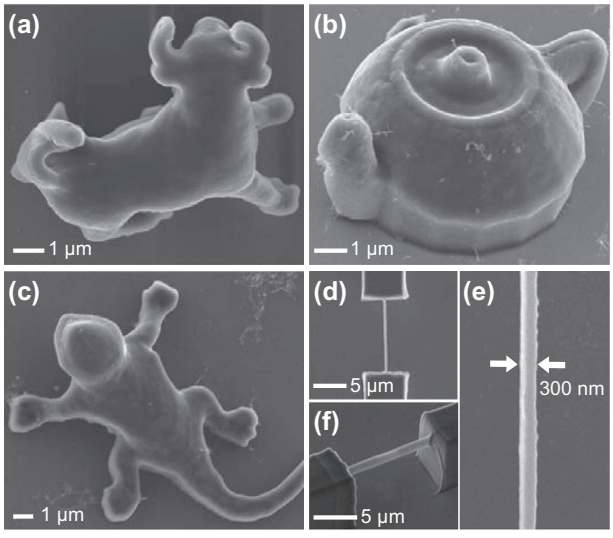

Fig. 2 – 3D micro/nano structural SWCNT/polymer composites are fabricated by using the TPP lithography. The structures in (a)–(f) are a 8-μm-long micro bull, a micro tea pod, a micro lizard, a nanowire suspended between two micro boxes, magnified image of (d), and perspective view of the nanowire, respectively.

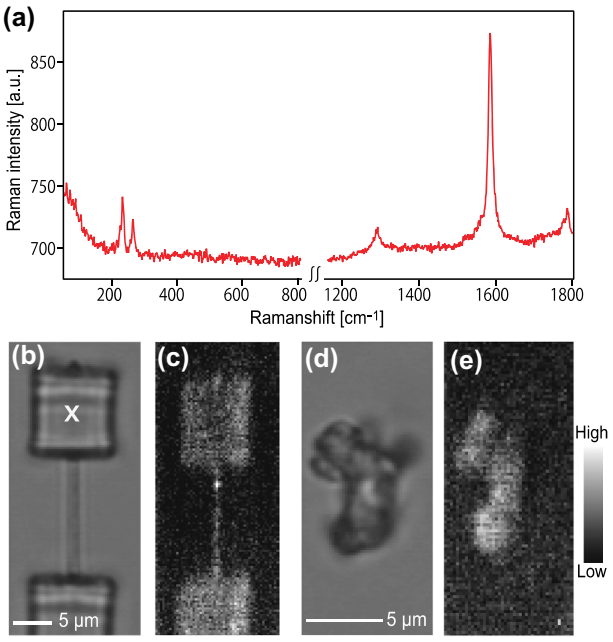

Fig. 3 – (a) A Raman spectrum taken from the box suspending the nanowire with an excitation wavelength of 785 nm. Laser power and exposure time are 2.8 mW and 60 s, respectively. (b) A bright field image of the 300-nm-thick nanowire suspended between two boxes. (c) A G-band Raman image taken at the same area in (b). Laser power and exposure time are 1.4 mW and 10 s, respectively. (d) A bright field image of a 8-μm-long micro bull. (e) A G-band Raman image taken at the same area in (d). Laser power and exposure time are 2.8 mW and 10 s, respectively.

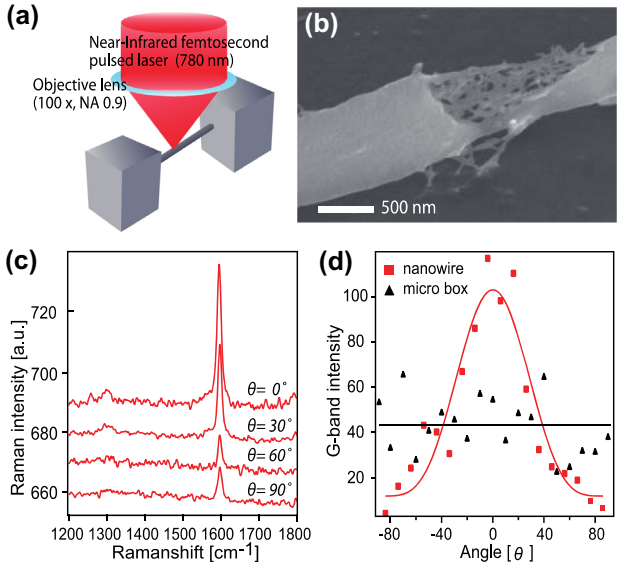

Fig. 4 – (a) A schematic setup for laser ablation. (b) SEM image at a clack produced by laser ablation. (c) Polarized Raman spectra of a 460-nm-wide-nanowire taken at different angles θ between polarization of the incident laser light and the nanowire axis. Excitation wavelength, laser power and exposure time are 785 nm, 0.6 mW and 10 s, respectively. (d) The angular dependence of G-band intensity. The square and triangle dots are experimental results for the nanowire and the box, respectively. The line is a $\cos^4\theta$ fitting curve for the nanowire [47].

SWCNTs in the structures. The Raman images of SWCNTs match the shapes of corresponding structures, indicating that SWCNTs are uniformly distributed throughout the whole structures, even in the nanowires.

To directly observe the inside of the SWCNT/polymer composites, laser ablation was performed to produce cracks on the structures (Fig. 4). A femtosecond pulsed laser beam with a wavelength of 780 nm was focused onto various structures with an intensity of ~45 GW/cm^2, which is much higher than the intensity for TPP, resulting in ablation of the polymer (Fig. 4a). As an example, a SEM picture of a 500-nm-wide nanowire suspended between two boxes after laser irradiation is shown in Fig. 4b. This picture shows entangled SWCNT-bundles with diameters of ~50 nm bridged between the crack of the polymer wire. It should be noted that the SWCNT-bundles are fully packed into the nanowire. Another interesting point to note is that the polymer was ablated more easily compared to SWCNTs, presumably due to the higher thermal stability of SWCNTs compared to that of the polymer. Furthermore, the picture in Fig. 4b seems to indicate that the SWCNTs inside the nanowire are aligned along the nanowire axis. Inspired by this intriguing result, we investigated the alignment of SWCNTs in the nanowire using polarized Raman spectroscopy. Polarized Raman spectroscopy was carried out on a 460-nm-wide nanowire with the polarizations of both incident and scattered light parallel to the nanowire axis [41]. Fig. 4c displays Raman spectra taken at different angles θ between the polarization of the incident laser light and the nanowire axis. Both the G-band and D-band peaks significantly vary in intensity as a function of θ. The angular dependence of the G-band intensity is plotted in Fig. 4d. The G-band intensity becomes largest when the polarization of the laser beam is parallel to the nanowire axis, while it becomes smallest when the polarization is perpendicular. This result clearly indicates that the SWCNTs are uniaxially aligned inside the wire. As a reference, the angular dependence of the box is also plotted in Fig. 4d. No angular dependence is observed, indicating that SWCNTs are randomly oriented in the boxes. The alignment of SWCNTs inside the wire probably arises from spatial confinement in the nanowire and/or volume shrinkage of polymer during the rinse and dry processes [42,43]. The alignment is expected to enhance the performances of mechanical properties of SWCNT/polymer composites [44]. The alignment would also provide significant enhancement of electrical conductivity [45,46], resulting from the effective creation of conductive nanotube network inside the wire, as seen in Fig. 4b.

To assess the spatial resolution of the fabrication technique, the nanowire width in lateral direction was measured as a function of laser intensity, and the wire width without

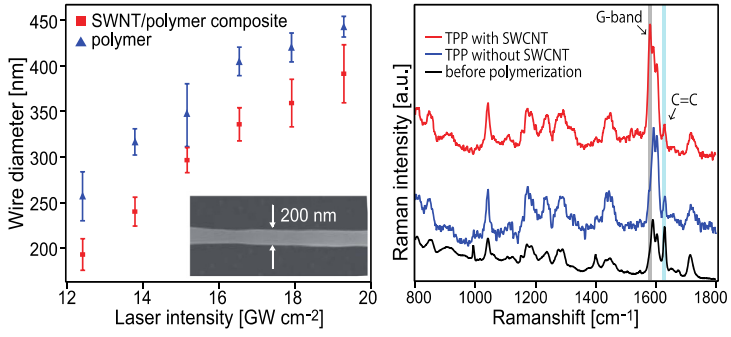

Fig. 5 – (a) The spatial resolution, which is estimated from wire width, as a function of laser intensity. Wire widths of SWCNT/polymer composites and those of polymer are indicated by the square and the triangle, respectively. (Inset) SEM image of a 200-nm-wide nanowire made of SWCNT/polymer composites. (b) Raman spectra of (black) photo-resin without SWCNTs, (blue) a micro box fabricated by TPP without SWCNTs, and (red) a micro box fabricated by TPP with SWCNTs. Excitation wavelength, laser power, and exposure time are 532 nm, 0.9 mW, and 120 s, respectively.

SWCNTs was also measured for comparison (Fig. 5a). The wire width decreased as the incident laser intensity was decreased, and the minimum width was around 200 nm when the average laser intensity was 12.4 GW/cm^2 (Fig. 5a inset). This means that the spatial resolution for fabrication is in the sub-micrometer regime. Moreover, the spatial resolution for the composites was higher than that for the resin without SWCNTs. One of the possible reasons for this result is that the incident photon was absorbed and dissipated by SWCNTs, and thus the effective laser intensity for TPP became lower. Another possibility is that SWCNTs would produce a radical quencher in the photo-resin that terminates the chain reaction of the photopolymerization. It is reported that SWCNTs deactivate singlet oxygen and produce triplet oxygen via energy transfer from singlet oxygen to SWCNTs [48]. If this effect occurs in our photo-resin, the presence of SWCNTs would lead to higher spatial resolution because triplet oxygen plays a role as a radical quencher in photopolymerization reaction [49].

To confirm the polymerization reactions of the photo-resin in the presence of SWCNTs, Raman spectra were taken with an excitation wavelength of 532 nm. A Raman spectrum of a micro box fabricated by TPP with SWCNTs is shown in Fig. 5b. A Raman spectrum of the photo-resin without SWCNTs and that of a micro box fabricated by TPP without SWCNTs are also shown, as a reference. Raman scattering signal from the polymer is observed under 532 nm excitation as well as the G-band signal from SWCNTs. The peak at 1640 cm^{-1} is assigned to C=C bond in the acrylate monomer [50]. After TPP, the peak intensity decreased in both TPP cases with and without SWCNTs. The result indicates that the polymerization reaction of the photo-resin proceeded smoothly even in the presence of SWCNTs.

4. Summary

We have demonstrated a method for 3D micro/nano-fabrication of SWCNT/polymer composites by TPP lithography. We showed that SWCNTs were fully and uniformly embedded into micro/nano-structures. In addition, we found that SWCNTs were aligned along the nanowire axis. Furthermore, the spatial resolution for fabrication was as small as 200 nm in lateral direction, which is much higher than that reported for other fabrication processes for the 3D structural composites [17]. The resultant structures would exhibit higher mechanical and electrical properties, especially in nanowire shaped composites, due to the self-alignment of SWCNTs inside the wire. These results indicate that our method is promising for realizing SWCNT/polymer composite-based 3D MEMS and NEMS.

Acknowledgement

This research is supported by The Canon Foundation, and KAKENHI Grant-in-Aid for Young Scientists (No. 21686010, 19810012), MEXT, Japan. P.K. and J.K. acknowledge financial support from the National Science Foundation through Grant No. OISE-0968405.

Appendix A. Supplementary data

Supplementary data associated with this article can be found, in the online version, at http://dx.doi.org/10.1016/j.carbon.2013.03.020.

REFERENCES

[1] Krishnan A, Dujardin E, Ebbesen TW, Yianilos PN, Treacy MMJ. Young's modulus of single-walled nanotubes. Phys Rev B 1998;58(20):14013–9.
[2] Tans SJ, Devoret MH, Dai H, Thess A, Smalley RE, Geerligs LJ, et al. Individual single-wall carbon nanotubes as quantum wires. Nature 1997;386(3):474–7.
[3] Hone J, Batlogg B, Benes Z, Johnson AT, Fischer JE. Quantized phonon spectrum of single-wall carbon nanotubes. Science 2000;289(8):1730–3.
[4] Bachilo SM, Strano MS, Kittrell C, Hauge RH, Smalley RE, Weisman RB. Structure-assigned optical spectra of single-walled carbon nanotubes. Science 2002;298(20):2361–6.
[5] Ci L, Suhr J, Pushparaj V, Zhang X, Ajayan PM. Continuous carbon nanotube reinforced composites. Nano Lett 2008;8(9):2762–6.
[6] Ramasubramaniam R, Chen J, Liu H. Homogeneous carbon nanotube/polymer composites for electrical applications. Appl Phys Lett 2003;83(14):2928–30.
[7] Biercuk MJ, Llaguno M, Radosavljevic M, Hyun JK, Johnson AT, Fischer JE. Carbon nanotube composites for thermal management. Appl Phys Lett 2002;80(15):2767–9.
[8] Ahir SV, Terentjev EM. Photomechanical actuation in polymer–nanotube composites. Nat Mater 2005;4:491–5.
[9] Park C, Kang JH, Harrison JS, Costen RC, Lowther SE. Actuating single wall carbon nanotube–polymer composites: intrinsic unimorphs. Adv Mater 2008;20(11):2074–9.
[10] An KH, Jeong SY, Hwang HR, Lee YH. Enhanced sensitivity of a gas sensor incorporating single-walled carbon nanotube–polypyrrole nanocomposites. Adv Mater 2004;16(12):1005–9.
[11] Shoji S, Suzuki H, Zaccaria RP, Sekkat Z, Kawata S. Optical polarizer made of uniaxially aligned short single-wall carbon nanotubes embedded in a polymer film. Phys Rev B 2008;77(15):153407-1–4.
[12] Vigolo B, Pénicaud A, Coulon C, Sauder C, Pailler R, Journet C, et al. Macroscopic fibers and ribbons of oriented carbon nanotubes. Science 2000;290(17):1331–4.
[13] Ko F, Gogotsi Y, Ali A, Naguib N, Ye H, Yang G, et al. Electrospinning of continuous carbon nanotube-filled nanofiber yarns. Adv Mater 2003;15(14):1161–5.
[14] Jin L, Bower C, Zhou O. Alignment of carbon nanotubes in a polymer matrix by mechanical stretching. Appl Phys Lett 1998;73(9):1197–9.
[15] Jin Z, Pramoda KP, Xu G, Goh SH. Dynamic mechanical behavior of melt-processed multi-walled carbon nanotube/poly(methyl methacrylate) composites. Chem Phys Lett 2001;337(1–3):43–7.
[16] Ajayan PM, Stephan O, Colliex C, Trauth D. Aligned carbon nanotube arrays formed by cutting a polymer resin–nanotube composite. Science 1994;265(26):1212–4.
[17] Lebel LL, Aissa B, Khakani MAE, Therriault D. Ultraviolet-assisted direct-write fabrication of carbon nanotube/polymer nanocomposite microcoils. Adv Mater 2010;22(5):592–6.
[18] Maruo S, Nakamura O, Kawata S. Three-dimensional microfabrication with two-photon-absorbed photopolymerization. Opt Lett 1997;22(2):132–4.
[19] Kawata S, Sun HB, Tanaka T, Takada K. Finer features for functional microdevices. Nature 2001;412(16):697–8.

[20] Kaneko K, Sun HB, Duan XM, Kawata S. Submicron diamond-lattice photonic crystals produced by two-photon laser nanofabrication. Appl Phys Lett 2003;83(11):2091–3.
[21] Deubel M, Freymann GV, Wegener M, Pereira S, Busch K, Soukoulis CM. Direct laser writing of three-dimensional photonic-crystal templates for telecommunications. Nat Mater 2004;3:444–7.
[22] Ledermann A, Cademartiri L, Hermatschweiler M, Toninelli C, Ozin GA, Wiersma DS, et al. Three-dimensional silicon inverse photonic quasicrystals for infrared wavelengths. Nat Mater 2006;5:942–5.
[23] Rill MS, Plet C, Thiel M, Staude I, Freymann GV, Linden S, et al. Photonic metamaterials by direct laser writing and silver chemical vapour deposition. Nat Mater 2008;7:543–6.
[24] Ergin T, Stenger N, Brenner P, Pendry JB, Wegener M. Three-dimensional invisibility cloak at optical wavelengths. Science 2010;328(5976):337–9.
[25] Kadic M, Bückmann T, Stenger N, Thiel M, Wegener M. On the practicability of pentamode mechanical metamaterials. Appl Phys Lett 2012;100(19):191901–4.
[26] Maruo S, Inoue H. Optically driven micropump produced by three-dimensional two-photon microfabrication. Appl Phys Lett 2006;89(14):144101–3.
[27] Maruo S, Ikuta K, Korogi H. Submicron manipulation tools driven by light in a liquid. Appl Phys Lett 2003;82(1):133–5.
[28] Tayalia P, Mendonca CR, Baldacchini T, Mooney DJ, Mazur E. 3D cell-migration studies using two-photon engineered polymer scaffolds. Adv Mater 2008;20(23):4494–8.
[29] Cumpston BH, Ananthavel SP, Barlow S, Dyer DL, Ehrlich JE, Erskine LL, et al. Two-photon polymerization initiators for three-dimensional optical data storage and microfabrication. Nature 1999;398(4):51–4.
[30] Ishitobi H, Shoji S, Hiramatsu T, Sun HB, Sekkat Z, Kawata S. Two-photon induced polymer nanomovement. Opt Exp 2008;16(18):14106–14.
[31] Sun ZB, Dong XZ, Nakanishi S, Chen WQ, Duan XM, Kawata S. Log-pile photonic crystal of CdS–polymer nanocomposites fabricated by combination of two-photon polymerization and in situ synthesis. Appl Phys A 2007;86(4):427–31.
[32] Sun ZB, Dong XZ, Chen WQ, Nakanishi S, Duan XM, Kawata S. Multicolor polymer nanocomposites: in situ synthesis and fabrication of 3D microstructures. Adv Mater 2008;20(5):914–9.
[33] Kuo WS, Lien CH, Cho KC, Chang CY, Lin CY, Huang LLH, et al. Multiphoton fabrication of freeform polymer microstructures with gold nanorods. Opt Exp 2010;18(26):27550–9.
[34] Masui K, Shoji S, Asaba K, Rodgers TC, Jin F, Duan XM, et al. Laser fabrication of Au nanorod aggregates microstructures assisted by two-photon polymerization. Opt Exp 2011;19(23):22786–96.
[35] Xia H, Wang J, Tian Y, Chen QD, Du XB, Zhang YL, et al. Ferrofluids for fabrication of remotely controllable micro-nanomachines by two-photon polymerization. Adv Mater 2010;22(29):3204–7.
[36] Tian Y, Zhang YL, Ku JF, He Y, Xu BB, Chen QD, et al. High performance magnetically controllable microturbines. Lab Chip 2010;10(21):2902–5.
[37] Liao M, Hishita S, Watanabe E, Koizumi S, Koide Y. Suspended single-crystal diamond nanowires for high-performance nanoelectromechanical switches. Adv Mater 2010;22(47):5393–7.
[38] Fujigaya T, Haraguchi S, Fukumaru T, Nakashima N. Development of novel carbon nanotube/photopolymer nanocomposites with high conductivity and their application to nanoimprint photolithography. Adv Mater 2008;20(11):2151–5.
[39] Thess A, Lee R, Nikolaev P, Dai H, Petit P, Robert J, et al. Crystalline ropes of metallic carbon nanotubes. Science 1996;273(26):483–7.
[40] O'Connell MJ, Bachilo SM, Huffman CB, Moore VC, Strano MS, Haroz EH, et al. Band gap fluorescence from individual single-walled carbon nanotubes. Science 2002;297(26):593–6.
[41] Duesberg GS, Loa I, Burghard M, Syassen K, Roth S. Polarized Raman spectroscopy on isolated single-wall carbon nanotubes. Phys Rev Lett 2000;85(25):5436–9.
[42] Li Y, Qi F, Yang H, Gong Q, Dong X, Duan X, et al. Nonuniform shrinkage and stretching of polymerized nanostructures fabricated by two-photon polymerization. Nanotechnology 2008;19(5):055303-1–5.
[43] Takada K, Wu D, Chen QD, Shoji S, Xia H, Kawata S, et al. Size-dependent behaviors of femtosecond laser-phototyped polymer micronanowires. Opt Lett 2009;34(5):566–8.
[44] Blighe FM, Young K, Vilatela JJ, Windle AH, Kinloch IA, Deng L, et al. The effect of nanotube content and orientation on the mechanical properties of polymer–nanotube composite fibers: separating intrinsic reinforcement from orientational effects. Adv Funct Mater 2011;21(2):364–71.
[45] Du F, Fischer JE, Winey KI. Effect of nanotube alignment on percolation conductivity in carbon nanotube/polymer composites. Phys Rev B 2005;72(12):121404-1–4.
[46] Shen J, Champagne MF, Gendron R, Guo S. The development of conductive carbon nanotube network in polypropylene-based composites during simultaneous biaxial stretching. Eur Polym J 2012;48(5):930–9.
[47] Jorio A, Souza Filho AG, Brar VW, Swan AK, Ünlü MS, Goldberg BB, et al. Polarized resonant Raman study of isolated single-wall carbon nanotubes: symmetry selection rules, dipolar and multipolar antenna effects. Phys Rev B 2002;65(12):121402–4.
[48] Lebedkin S, Kareev I, Hennrich F, Kappes MM. Efficient quenching of singlet oxygen via energy transfer to semiconducting single-walled carbon nanotubes. J Phys Chem C 2008;112(42):16236–9.
[49] Takada K, Sun HB, Kawata S. Improved spatial resolution and surface roughness in photopolymerization-based laser nanowriting. Appl Phys Lett 2005;86(7):071122–3.
[50] Yang J, Mei Y, Hook AL, Taylor M, Urquhart AJ, Bogatryrev SR, et al. Polymer surface functionalities that control human embryoid body cell adhesion revealed by high throughput surface characterization of combinational material microarrays. Biomaterials 2010;31(34):8827–38.